ACS APPLIED OPTICAL MATERIALS

Guided Self-Assembly of DNA Tiles into One- and Two-Dimensional Patterns Using Strand-Displacement and Optochemical Pathways

Devanathan Perumal, Qi Yang, Maciej Jeziorek, Jung Yeon Lee, Jean-Pierre Etchegaray, and Fei Zhang*

Cite This: https://doi.org/10.1021/acsaom.3c00473

Read Online

ACCESS | Metrics & More | Article Recommendations | Supporting Information

ABSTRACT: Self-assembly is a key process in living systems to facilitate the formation of intricate structures of biomolecules with properties vital to biological functions. In engineered systems, controlling self-assembly in response to external stimuli is crucial for leveraging biomolecular behaviors for technological applications. In this study, we present two approaches to direct the linear growth and 2D self-assembly of DNA tiles. The first strategy involves using toehold-mediated strand-displacement reactions. The second approach employs a photoresponsive duplex module, which contains a tile-activator strand coupled with a complementary strand that incorporates a photocleavable *o*-nitrobenzyl group. Exposure to UV light triggers the cleavage of this photocleavable linker, destabilizing the duplex module and releasing the activator strand, resulting in activation of the DNA-tile assembly. This guided self-assembly in DNA-based systems demonstrates new potential in developing biosensors, molecular machines, and targeted drug delivery.

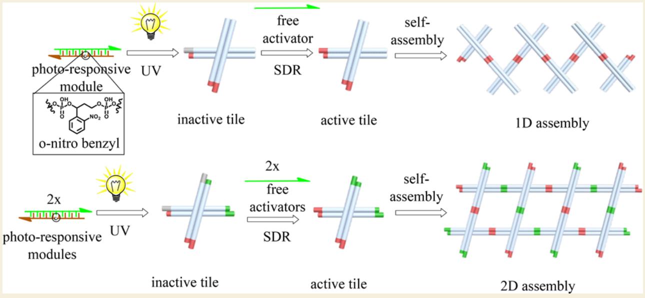

KEYWORDS: *double-crossover DNA tiles, self-assembly, optochemical trigger, photocleavage, DNA strand displacement*

1. INTRODUCTION

Responsive self-assembly plays a crucial role in many biological processes[1,2] such as microtubule formation[3] and enzyme phosphorylation,[4] where complexity and high spatiotemporal control are required.[5,6] Applying this responsive self-assembly principle to create nanostructures that can respond dynamically and in a timely manner opens up potential applications in biosensing,[7−11] cell engineering,[12] and nanodevice fabrication.[13,14] DNA nanostructures, due to their high programmability, biocompatibility, and nanoscale dimension, are great candidates for constructing and studying responsive systems.[15−22] DNA has emerged as an excellent material for nanoengineering, with studies harnessing various external stimuli, such as enzymes,[23,24] nucleic acids,[25] small molecules,[26] light,[27] metal ions,[28,29] and pH,[30] to precisely control the self-assembly of DNA nanostructures. Among them, light has been proven to be an outstanding external trigger due to its nontoxicity, orthogonality, cell permeability, and spatiotemporal control capabilities.[31−35] Thus, optical switches and photolabile groups are at the forefront in regulating enzymes,[36,37] nucleic acids,[38] and small molecules.[39]

Photochemical regulation in DNA nanostructures typically involves single-stranded DNA (ssDNA) with photoresponsive groups to activate or inactivate their function.[40] This can be achieved by attaching light-responsive moieties to specified locations of a nucleotide, such as the phosphate backbone,[41] the sugar unit,[42] or the nucleobase.[43] The development of photoresponsive DNA nanostructures focuses on photoisomerization,[44−51] photocaging/photocleavage,[52,53] and photo-cross-linking.[54] These mechanisms trigger structural and functional alterations in DNA, enabling precise molecular-level self-assembly control. The following sections will delve into these categories, showing the varied ways that light impacts DNA-based materials.

Photoisomerization in DNA nanostructures involves integrating photoisomerizable functional groups, such as azobenzene, stilbene, spiropyran, and diarylethylene, into ssDNA, allowing reversible transformation between *E* and *Z* isomers with specific light wavelengths. This phenomenon has been harnessed to construct various dynamic DNA nanostructures.[55−58] For example, a light-controlled DNAzyme, featuring a *trans*-azobenzene-stabilized hairpin loop, transitions from an inactive to an active state under UV light.[55] This activation process unfolds the hairpin loop into a single strand, driven by the shift of *trans*-azobenzene units to the cis-isomer state, thereby enabling the reconfiguration. Similarly, a light-driven DNA walker has been created by using azobenzene units isomerized by distinct light frequencies.[56] Another innovative design mimics molecular rotaxane for cargo translocation,

Special Issue: Optical Applications of DNA Nanotechnology

Received: December 29, 2023
Revised: March 1, 2024
Accepted: March 4, 2024

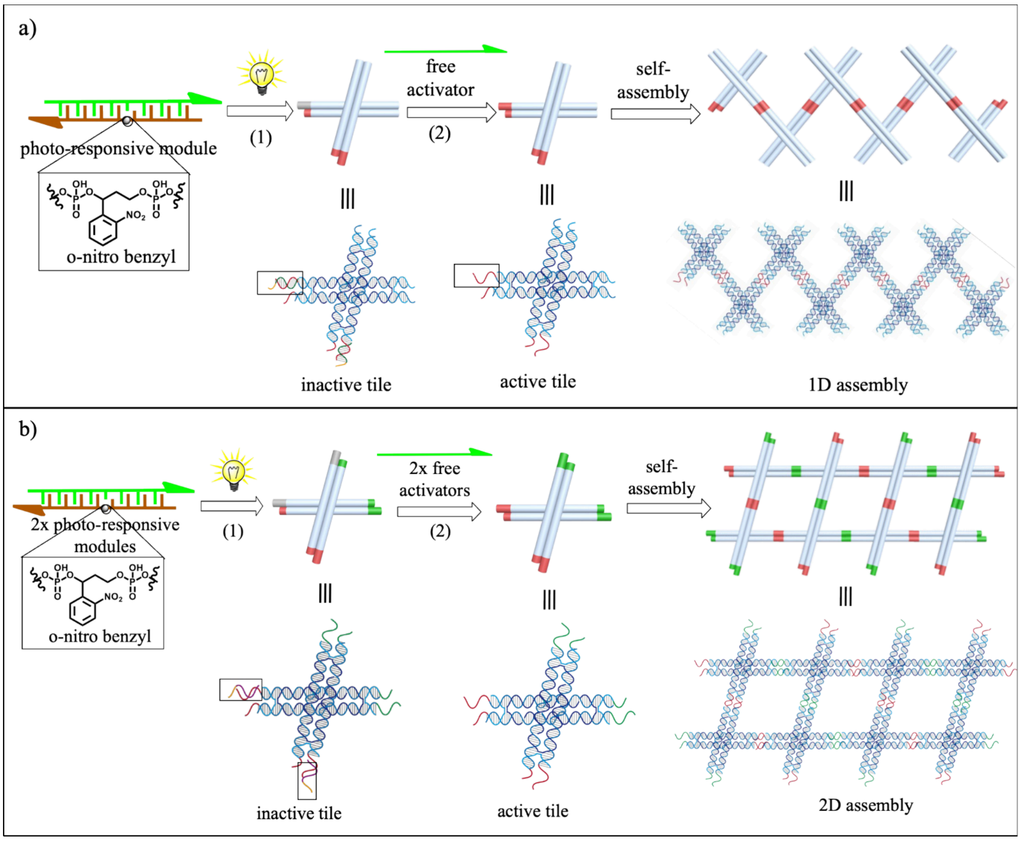

Figure 1. Schematics of the responsive self-assembly of (a) 1D and (b) 2D DNA tiles triggered by UV light (1) and a strand-displacement process (2). The release of the free activator strand (green) from the photoresponsive module guides the conversion of the inactive DNA tile (gray) to the active form (green) through a SDR that sequesters an inhibitor strand from the DNA tile. Active tiles then self-assemble into 1D and 2D structures.

utilizing light to trigger strand displacement.[57] Additionally, light-responsive DNA nanoscissors have been created, leveraging the reversible isomerization of azobenzene to control opening and closing actions.[58]

Incorporating photocleavable groups like *o*-nitrobenzyl and coumarin into nucleic acid allows for the temporary suspension of their function, which can be reactivated by light-triggered cleavage.[59,60] For instance, Tohgasaki and co-workers developed a DNA nanocapsule featuring a light-activated unlocking mechanism designed for delivering contents into cells.[61] This system utilizes a photocaging approach to regulate the capsule's opening upon exposure to light, enabling controlled intracellular delivery. Another example is a dynamic DNA nanotweezer with photocaged DNA strands inside.[62] The tweezer can be rapidly switched from a closed state to an open state when exposed to UV light, allowing photocages to release the lock between the tweezer arms and significantly increasing the distance between its arms.

Photo-cross-linking has been utilized to stabilize DNA nanostructures by employing agents like thymine, 8-methoxypsoralen, and cyanovinylcarbazole to link the ends of adjacent strands. Rajendran and colleagues utilized 8-methoxypsoralen for this purpose, achieving structures that remained stable even at high temperatures and showed improved assembly yield.[63] Similarly, the research groups employed 3-cyanovinylcarbazole[64] and thymidine,[65] respectively, placing these agents strategically within DNA nanostructures for effective cross-linking under UV light.

Inspired by these results, we developed two methods to precisely control the self-assembly of DNA tiles into one-dimensional (1D) and two-dimensional (2D) structures. One method uses toehold-mediated strand-displacement reactions (SDRs), while the other employs a photoresponsive duplex module activated by UV light to release an activator, initiating DNA-tile assembly. The exploitation of these methods will facilitate advanced developments in nanotechnology and biomaterials, enabling the creation of highly functionalized, programmable nanostructures.

2. RESULTS AND DISCUSSION

To demonstrate our approach, we employed a layered double-crossover DNA tile that was assembled through the hybridization of 12 different ssDNA strands,[66] exhibiting two pairs of arms with sticky ends that can be used for the formation of 1D and 2D assemblies. These DNA tiles were reported to form arrays through annealing, which is a temperature-programmed cooling process. To enable regulation of the assembly process by external stimuli, we redesigned the tiles to separate the monomer formation of individual tiles from the tile−tile interaction by adding extensions to the sticky ends. DNA tiles were first inactivated by an inhibitor strand that blocked one sticky strand, preventing interaction between tiles through hybridization. These inactive tiles were then able to be reactivated by directly supplying an activator strand that caused dissociation of the inhibitor from the tile via a toehold-mediated SDR. The release of the activator strand was programmed further to enable optochemical control of the DNA-tile self-assembly. We engineered a photoresponsive module that consisted of an activator strand, with its complementary strand containing a photocleavable *o*-nitro-

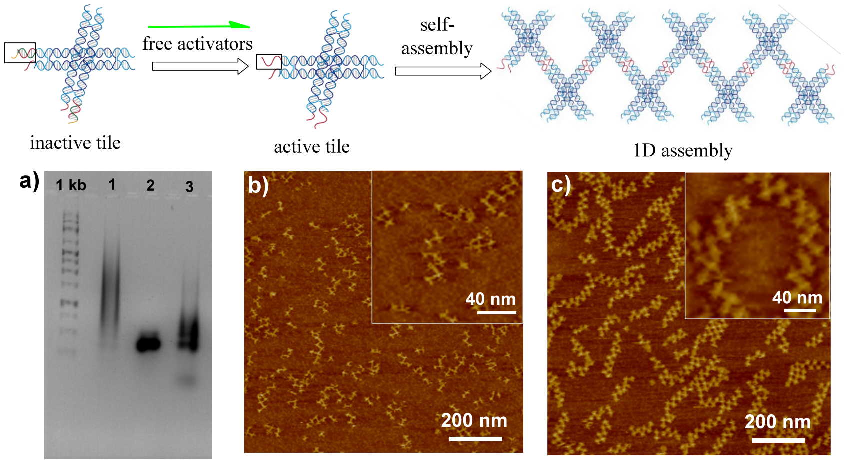

Figure 2. Responsive self-assembly of 1D DNA tiles via a SDR. (a) 1.5% AGE analysis of DNA tiles before and after tile activation with a free activator (lane 1, positive control; lane 2, inactive tile; lane 3, reactivated tile via a SDR). AFM images of the DNA-tile assembly (b) before and (c) after tile activation with the free activator.

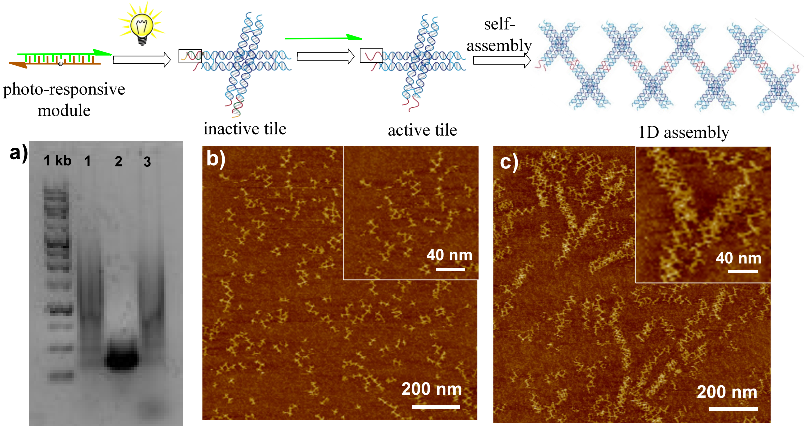

Figure 3. Responsive self-assembly of a 1D DNA tile triggered by UV light. (a) 1.5% AGE analysis of DNA tiles before and after UV-light shedding (lane 1, positive control; lane 2, inactive tile; lane 3, reactivated tile via an optochemical reaction). AFM images of DNA-tile assembly (b) before and (c) after UV treatment.

benzyl group. Upon exposure to UV light, cleavage of the *o*-nitrobenzyl linker occurred, destabilizing the duplex and releasing the activator strand. This resulted in sequential activation of the DNA tiles, demonstrating a controlled self-assembly pathway (Figure 1).

We began by showcasing the responsive 1D assembly activated by a SDR. Agarose gel electrophoresis (AGE) was performed to characterize the self-assembly of the inactive and active tiles. This is because the separation range of native gel is about 75−500 bp, while it is 200−4000 bp for 1.5% agarose gel. Inactive tiles were formed by annealing the corresponding ssDNA strands. Both the gel data and atomic force microscopy (AFM) images verified the formation of these well-defined monomer structures (Figure 2). Activation was initiated by adding activator DNA strands to the monomer mix and allowing the strands to incubate. AGE results revealed a distinct gel shift for the reactivated tiles compared to their inactive counterparts (Figure 2a). The electrophoretic band observed for the reactivated tiles was similar to that of the reference tile assembled without an inhibitor strand, working as the positive control of our experiments. Complementing the AGE findings, in-fluid AFM imaging also showed the formation of 1D assemblies from the reactivated tile via a SDR, which was similar to assemblies observed from the reference tiles (Figure S1). In contrast, for the inactivated tiles, only isolated monomer tiles were observed in the AFM analysis (Figure 2b). These results together suggest that our SDR method can effectively transform inactive tiles into active tiles for controlled self-assembly.

To demonstrate the light-responsive 1D assembly of DNA tiles, we integrated a photoresponsive duplex module with a photolabile group into the design of the inactive tiles. After UV irradiation, AGE analysis showed a clear band upshift for the reactivated tile, indicating inhibitor strand removal and subsequent tile activation (Figure 3a). The upshifted band for the UV-treated sample matched that of the reference tile, which was formed without an inhibitor and served as a positive control. Conversely, the non-UV-treated samples displayed only a monomer band. The light-responsive assembly of DNA tiles was further analyzed by AFM. In the absence of UV light, only monomer tiles were observed under AFM (Figure 3b), whereas in the presence of UV light, a significant number of 1D periodic assemblies were observed (Figure 3c). These 1D assemblies were comparable to the assembled structures obtained from the reference tile (Figure S1). The formation yields of 1D assemblies with more than five monomers of the reactivated tiles through SDR and light-responsive pathways closely matched that of the positive control (Figure S12 and Table S3). In support of this, fluorescence microscopic analysis also showed that UV light triggered the responsive assembly of Cy3-labeled DNA tiles (λ_{ex} = 530 nm). No significant Cy3 fluorescence was obtained in the case of inactive tiles due to the quenching effect of a Cy5-modified inhibitor (Figure S4). These results cohesively support our design principle that DNA-tile assembly can be precisely controlled via a noninvasive optochemical reaction.

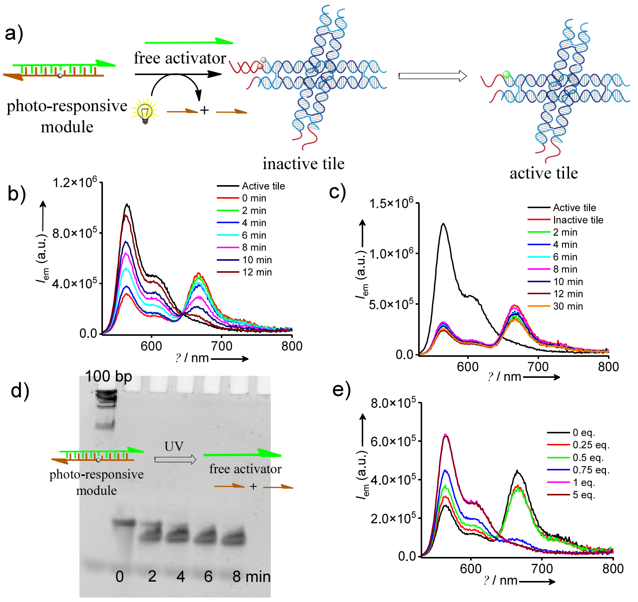

Figure 4. Light-responsive self-assembly of the 1D DNA tile triggered by UV light. (a) Schematic diagram showing the light-triggered release of a free activator from the photoresponsive module and UV dose-dependent fluorescence studies of (b) a photoresponsive module and (c) a nonresponsive module. (d) 12% native PAGE analyses showing the release of the free activator strand from a photoresponsive module (1 μM in 1xTAE, Mg^{2+}, pH 8.2) in UV dose-dependent manner. (e) Concentration-dependent fluorescence spectral studies with increasing concentration of a photoresponsive module. All of the fluorescence experiments shown in this panel were carried out at a 50 nM concentration of DNA tile in 1xTAE buffer, 12.5 mm $MgCl_2$ at pH 8.2, and 28 °C.

We then systematically studied the light-induced release of the activator using fluorescence experiments and native PAGE analyses (Figure 4a). To label the light-responsive module, one of the sticky strands and the inhibitor strand were tagged with a Cy3 fluorophore (λ_{ex} = 515 nm and λ_{em} = 550 nm) and a Cy5 quencher, respectively. As expected, the release rate of the 16-nucleotide-long activator strand from the light-responsive module followed a UV dose-dependent behavior. With only 5 min of UV treatment (UVP transilluminator, 365 nm), ∼50% of the activators were released, while it needed 8 min of light exposure to reach >90% release (Figure 4b). On the other hand, UV dose-dependent studies with a nonresponsive module, which lacked a photoresponsive linker, did not show tile activation under the same experimental conditions (Figure 4c). It is noted that the length of the light-responsive module is important. If it was extended from 16 to 24 nucleotides, no significant increase of the fluorescence intensity was observed, indicating that the activator was still firmly bound to the photoresponsive strand's halves due to the high melting temperature of the duplexes (Figure S9). Furthermore, native PAGE analyses were also employed to study the UV dose-dependent effect of the light-responsive module (Figure 4d). As predicted, the nonresponsive module, which is a duplex lacking a photocleavable linker, showed no remarkable changes in the electrophoretic mobility (Figure S11). To investigate the amount of activator required for tile activation, the fluorescence intensity recovery at 515 nm was collected as a function of the concentration of the light-responsive module. A steady increase in the fluorescence intensity was observed with increasing concentration of the light-responsive module and plateaued with 1 mol equiv of the activator (Figure 4e). A further increase of the light-responsive module concentration up to 5 mol equiv did not show any notable change in the fluorescence intensity. These observations demonstrated that the photoresponsive release of the DNA activator in this DNA-tile system is an efficient process with programmable behaviors.

To further prove the versatility of our design strategy, we demonstrated the responsive self-assembly of 2D DNA tiles using a SDR and light-controlled reaction. Like the 1D assemblies, we first studied the dynamics of responsive 2D assemblies using a SDR only. In the 2D assembly tile design, we redesigned the DNA tiles to carry two inhibitors on two of the four sets of sticky ends and thus to prevent the formation of 2D arrays. The activation of a previously inactivated tile through the addition of free activators via DNA strand substitution was confirmed by AGE and AFM analyses. It was clear from the AGE analysis that the inactive tile showed a much lower electrophoretic migration compared to the reactivated tile (Figure 5a), with the electrophoretic shift of the reactivated tile aligning with that of the reference tile. Similarly, AFM analysis also displayed the formation of 2D periodic assemblies in the reactivated tile (Figure 5c), whereas only monomer tiles were seen in the inactive tiles (Figure 5b). The 2D arrays identified via AFM closely resembled those formed by the reference tile without any inhibitors (Figure S5), indicating the successful restoration of tile activity. It is also to be noted that the size of the 2D arrays obtained in our studies is much smaller than that in previous work. We attribute this size difference to modification of the tile design and the change of annealing conditions. In order to incorporate the responsive strand, the sticky end domains of the original tiles were extended with ssDNA overhangs for the reversible binding of activator and inhibitor strands. In addition, the previous study used a one-pot annealing program to archive large arrays. However, in our study, we need to conduct a stepwise annealing program to first form inactive tiles, followed by the formation of active tiles with the addition of activator strands. Therefore, the relatively smaller size of the 2D assembly in our design is expected due to modification of the tile design and the change in annealing conditions.

Finally, to demonstrate the light-triggered assembly of DNA 2D arrays, a pair of photoresponsive modules carrying two different activator strands were introduced to the inactive tile systems. The release of free activators upon UV-light irradiation gradually initiated the tile assembly by sequestering the inhibitor strands responsible for tile inactivation. The result of AGE showed a notable difference in the electrophoretic migration rate of the tile before and after UV treatment (Figure 6a). The electrophoretic bands corresponding to the reactivated tile showed a migration rate similar to that of the reference tile, which was the positive control sample with 2D arrays assembled from inhibitor-free tiles. This was further

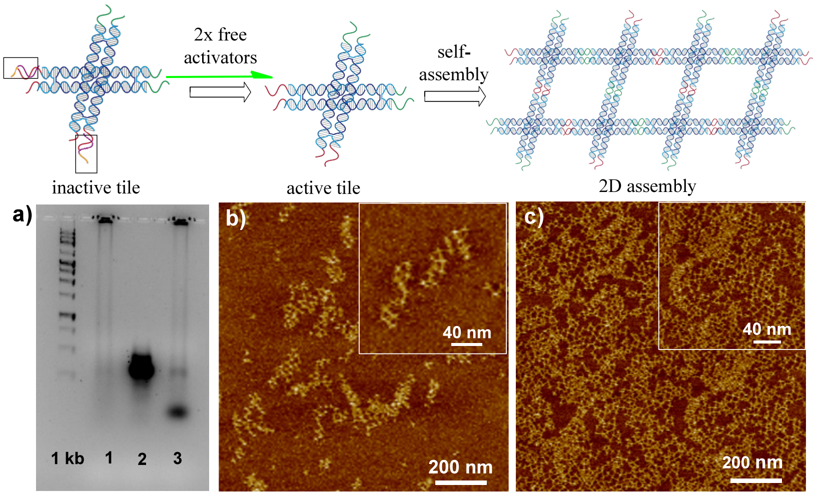

Figure 5. Responsive self-assembly of a 2D DNA tile via a SDR. (a) 1.5% AGE analysis of DNA tile before and after tile activation with free activators (lane 1, positive control; lane 2, inactive tile; lane 3, reactivated tile via a SDR). AFM images of DNA-tile assembly (b) before and (c) after tile activation with free activators.

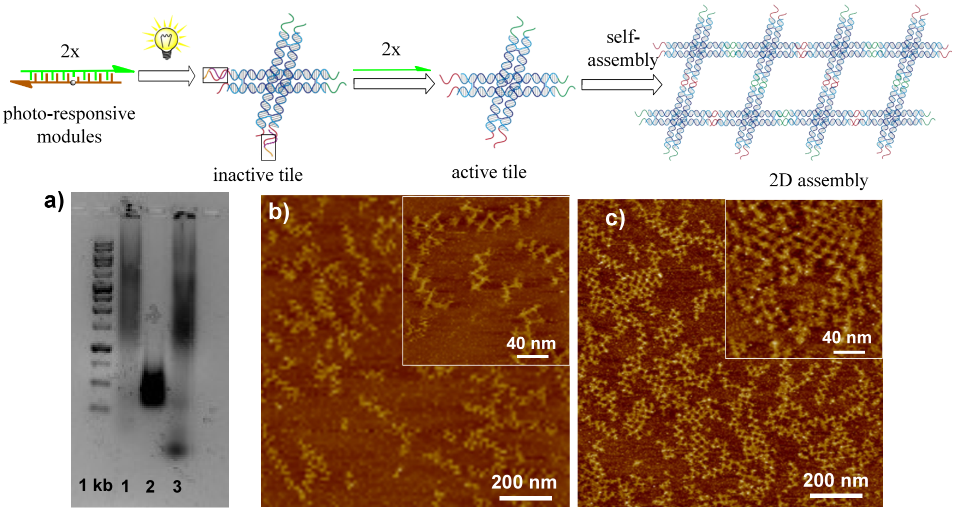

Figure 6. Responsive self-assembly of a 2D DNA tile triggered by UV light. (a) 1.5% AGE analysis of DNA tile before and after UV light shedding (lane 1, positive control; lane 2, inactive tiles; lane 3, reactivated tiles via an optochemical reaction). AFM images of DNA-tile assembly (b) before and (c) after UV treatment.

confirmed by AFM analysis, which also revealed the formation of 2D arrays for the UV-treated DNA samples (Figure 6c). No significant array formation was observed for the non-UV-treated DNA samples (Figure 6b). AFM analysis of the UV-treated samples was aligned with that of the reference tile assembled without inhibitor strands. Overall, these results demonstrated that the 2D self-assembly of DNA tiles can be precisely regulated through both strand substitution reactions and optochemical triggers.

3. CONCLUSIONS

In conclusion, our study demonstrated simple yet efficient approaches for initiating the 1D and 2D assembly of DNA tiles via SDR and optochemical mechanisms. Our strategies, characterized by their simplicity and efficiency, have the potential to be applied to various DNA-based systems including DNA origami. It opens avenues for developing advanced biosensors, light-driven nanomachines, and responsive nanocontainers. Its applications span from medical diagnostics and targeted drug-delivery systems, where precision and responsiveness are important, to the creation of smart materials that can change properties on demand for use in soft robotics and adaptive optics. In advancing this field, future research will focus on incorporating more stimuli-responsive elements, improving assembly accuracy, and scaling up these nanostructures for practical applications. We are particularly excited about designing light-responsive nanocarriers for the efficient and targeted delivery of RNA to living cells and developing rapid light-powered DNA nanodevices, highlighting our continued focus in these innovative areas.

■ ASSOCIATED CONTENT

Supporting Information

The Supporting Information is available free of charge at https://pubs.acs.org/doi/10.1021/acsaom.3c00473.

Experimental and characterization details of all designs and additional microscopic data (PDF)

■ AUTHOR INFORMATION

Corresponding Author

Fei Zhang − *Department of Chemistry, Rutgers University, Newark, New Jersey 07102, United States;* orcid.org/0000-0002-3177-7547; Email: fei.zhang@rutgers.edu

Authors

Devanathan Perumal − *Department of Chemistry, Rutgers University, Newark, New Jersey 07102, United States*
Qi Yang − *Department of Chemistry, Rutgers University, Newark, New Jersey 07102, United States*
Maciej Jeziorek − *Department of Biological Sciences, Rutgers University, Newark, New Jersey 07102, United States*
Jung Yeon Lee − *Department of Chemistry, Rutgers University, Newark, New Jersey 07102, United States*
Jean-Pierre Etchegaray − *Department of Biological Sciences, Rutgers University, Newark, New Jersey 07102, United States; Rutgers Cancer Institute of New Jersey, New Brunswick, New Jersey 08901, United States*

Complete contact information is available at:
https://pubs.acs.org/10.1021/acsaom.3c00473

Author Contributions

D.P. and F.Z. conceived the idea. D.P. and Q.Y. designed the structures. D.P., Q.Y., and J.Y.L. prepared the samples and characterized them through AGE and AFM. M.J. and D.P. performed the fluorescence microscopic study. All authors performed data analysis. The manuscript was written through contributions of all authors. All authors have given approval to the final version of the manuscript.

Notes

The authors declare no competing financial interest.

■ ACKNOWLEDGMENTS

This work is supported by a U.S. National Science Foundation Faculty Early Career Development Award (DMR-2046835) and a faculty startup fund from Rutgers University.

■ REFERENCES

(1) Varela, F.; Maturana, H.; Uribe, R. Autopoiesis: The organization of living systems, its characterization, and a model. *Biosystems* **1974**, *5*, 187−196.

(2) Fleischaker, G. Autopoiesis: the status of its system logic. *Biosystems* **1988**, *22*, 37−49.

(3) Lingrel, J. B.; Kuntzweiler, T. Na$^+$, K$^{(+)}$ -ATPase. *J. Biol. Chem.* **1994**, *269*, 19659−19662.

(4) Conde, C.; Cáceres, A. Microtubule assembly, organization and dynamics in axons and dendrites. *Nat. Rev. Neurosci.* **2009**, *10*, 319−332.

(5) Karsenti, E. Self-organization in cell biology: a brief history. *Nature Rev. Mol. Cell Biol.* **2008**, *9*, 255−262.

(6) Nitschke, J. R. Systems chemistry: molecular networks come of age. *Nature* **2009**, *462*, 736−738.

(7) Lin, L.; Zhao, H.; Li, J.; Tang, J.; Duan, M.; Jiang, L. Study on colloidal Au-enhanced DNA sensing by quartz crystal microbalance. *Biochem. Biophys. Res. Commun.* **2000**, *274*, 817−820.

(8) Turner, M.; Golovko, V. B.; Vaughan, O. P. H.; Abdulkin, P.; Berenguer-Murcia, A.; Tikhov, M. S.; Johnson, B. F. G.; Lambert, R. M. Selective oxidation with dioxygen by gold nanoparticle catalysts derived from 55-Atom clusters. *Nature* **2008**, *454*, 981−983.

(9) Zhang, J.; Boghossian, A. A.; Barone, P. W.; Rwei, A.; Kim, J.-H.; Lin, D.; Heller, D. A.; Hilmer, A. J.; Nair, N.; Reuel, N. F.; Strano, M. S. Single molecule detection of nitric oxide enabled by d(AT) 15 DNA adsorbed to near infrared fluorescent single-walled carbon nanotubes. *J. Am. Chem. Soc.* **2011**, *133*, 567−581.

(10) Hai, Z.; Liang, G. Intracellular self-assembly of nanoprobes for molecular imaging. *Adv. Biosyst.* **2018**, *2*, No. 1800108.

(11) Mannoor, M. S.; Tao, H.; Clayton, J. D.; Sengupta, A.; Kaplan, D. L.; Naik, R. R.; Verma, N.; Omenetto, F. G.; McAlpine, M. C. Graphene-based wireless bacteria detection on tooth enamel. *Nat. Commun.* **2012**, *3*, 763.

(12) Nielsen, J.; Keasling, J. D. Engineering cellular metabolism. *Cell* **2016**, *164*, 1185−1197.

(13) Bath, J.; Turberfield, A. J. DNA nanomachines. *Nat. Nanotechnol.* **2007**, *2*, 275−284.

(14) Krishnan, Y.; Simmel, F. C. Nucleic acid-based molecular devices. *Angew. Chem., Int. Ed.* **2011**, *50*, 3124−3156.

(15) Seeman, N. C. Nucleic acid junctions and lattices. *J. Theor. Biol.* **1982**, *99*, 237−247.

(16) Zheng, J.; Birktoft, J. J.; Chen, Y.; Wang, T.; Sha, R.; Constantinou, P. E.; Ginell, S.; Mao, C.; Seeman, N. C. From molecular to macroscopic via the rational design of a self-assembled 3D DNA crystal. *Nature* **2009**, *461*, 74−77.

(17) Qian, L.; Winfree, E.; Bruck, J. Neural network computation with DNA strand displacement cascades. *Nature* **2011**, *475*, 368−372.

(18) Zhang, D. Y.; Seelig, G. Dynamic DNA nanotechnology using strand-displacement reactions. *Nat. Chem.* **2011**, *3*, 103−113.

(19) Yurke, B. A.; Turberfield, A. J.; Mills, A. P. J.; Simmel, F. C.; Neumann, J. L. A DNA-fueled molecular machine made of DNA. *Nature* **2000**, *406*, 605−608.

(20) Liu, D.; Balasubramanian, S. A proton-fueled DNA nanomachine. *Angew. Chem., Int. Ed.* **2003**, *42*, 5734−5736.

(21) Yin, P.; Yan, H.; Daniell, X. G.; Turberfield, A. J.; Reif, J. H. A unidirectional DNA walker that moves autonomously along a track. *Angew. Chem., Int. Ed.* **2004**, *43*, 4906−4911.

(22) Yang, Q.; Chang, X.; Lee, J. Y.; Olivera, T. R.; Saji, M.; Wisniewski, H.; Kim, S.; Zhang, F. Recent advances in self-assembled DNA nanostructures for bioimaging. *ACS Appl. Bio Mater.* **2022**, *5* (10), 4652−4667.

(23) Agarwal, S.; Franco, E. Enzyme-driven assembly, and disassembly of hybrid DNA−RNA nanotubes. *J. Am. Chem. Soc.* **2019**, *141*, 7831−7841.

(24) Wilner, O. I.; Weizmann, Y.; Gill, R.; Lioubashevski, O.; Freeman, R.; Willner, I. Enzyme cascades activated on topologically programmed DNA scaffolds. *Nat. Nanotechnol.* **2009**, *4*, 249−254.

(25) Willner, I.; Shlyahovsky, B.; Zayats, M.; Willner, B. DNAzymes for sensing, nanobiotechnology and logic gate applications. *Chem. Soc. Rev.* **2008**, *37*, 1153−1165.

(26) Del Grosso, E.; Prins, L. J.; Ricci, F. Transient DNA-Based Nanostructures Controlled by Redox Inputs. *Angew. Chem., Int. Ed.* **2020**, *59*, 13238−13245.

(27) Chen, Y.; Wang, Z.; He, Y.; Yoon, Y. J.; Jung, J.; Zhang, G.; Lin, Z. Light−enabled reversible self−assembly and tunable optical properties of stable hairy nanoparticles. *Proc. Natl. Acad. Sci. U.S.A.* **2018**, *115*, E1391−E1400.

(28) Wang, Z. G.; Elbaz, J.; Willner, I. DNA machines: bipedal walker and stepper. *Nano Lett.* **2011**, *11*, 304−309.

(29) Miyake, Y.; Togashi, H.; Tashiro, M.; Yamaguchi, H.; Oda, S.; Kudo, M.; Tanaka, Y.; Kondo, Y.; Sawa, R.; Fujimoto, T.; Machinami, T.; Ono, A. Mercury II-mediated formation of thymine−HgII−thymine base pairs in DNA duplexes. *J. Am. Chem. Soc.* **2006**, *128*, 2172−2173.

(30) Qi, X. J.; Lu, C. H.; Liu, X.; Shimron, S.; Yang, H. H.; Willner, I. Autonomous control of interfacial electron transfer and the activation of DNA machines by an oscillatory pH system. *Nano Lett.* **2013**, *13*, 4920−4924.

(31) Lin, M.; Yi, X.; Wan, H.; Zhang, J.; Huang, F.; Xia, F. Photo responsive electrochemical DNA biosensors achieving various dynamic ranges by using only-one capture probe. *Anal. Chem.* **2020**, *92* (14), 9963−9970.

(32) Liu, Q.; Deiters, A. Optochemical control of deoxy oligonucleotide function via a nucleobase-caging approach. *Acc. Chem. Res.* **2014**, *47* (1), 45−55.

(33) Chu, H.; Zhao, J.; Mi, Y.; Zhao, Y.; Li, L. Near-infrared light-initiated hybridization chain reaction for spatially and temporally resolved signal amplification. *Angew. Chem., Int. Ed.* **2019**, *58*, 14877−14881.

(34) Kohman, R. E.; Cha, S. S.; Man, H. Y.; Han, X. Light-Triggered Release of Bioactive Molecules from DNA Nanostructures. *Nano Lett.* **2016**, *16*, 2781−2785.

(35) Jin, C.; Liu, X.; Bai, H.; Wang, R.; Tan, J.; Peng, X.; Tan, W. Engineering stability-tunable DNA micelles using photo-controllable dissociation of an intermolecular G-Quadruplex. *ACS Nano* **2017**, *11*, 12087−12093.

(36) Sumaoka, J.; Kawata, K.; Komiyama, M. Photo-regulation of RNA hydrolysis by the Zinc(ii) complex carrying azobenzene. *Chem. Lett.* **1999**, *28* (5), 439−440.

(37) Gu, Y.; Wu, X.; Liu, H.; Pan, Q.; Chen, Y. Photo switchable Heparinase III for enzymatic preparation of low molecular weight heparin. *Org. Lett.* **2018**, *20* (1), 48−51.

(38) Anhäuser, L.; Klöcker, N.; Muttach, F.; Mäsing, F.; Špaček, P.; Studer, A.; Rentmeister, A. A benzophenone-based photocaging strategy for the N7 position of guanosine. *Angew. Chem., Int. Ed.* **2020**, *59*, 3161−3165.

(39) Song, G.; Heng, H.; Wang, J.; Liu, R.; Huang, Y.; Lu, H.; Du, K.; Feng, F.; Wang, S. Photoactivated in situ generation of near infrared cyanines for spatiotemporally controlled fluorescence imaging in living cells. *Angew. Chem., Int. Ed.* **2021**, *60*, 16889−16893.

(40) Lubbe, A. S.; Szymanski, W.; Feringa, B. L. Recent developments in reversible photoregulation of oligonucleotide structure and function. *Chem. Soc. Rev.* **2017**, *46*, 1052−1079.

(41) Lewis, F. D.; Liu, X. Photo triggered DNA hairpin formation in a stilbene diether-linked bis(oligonucleotide) conjugate. *J. Am. Chem. Soc.* **1999**, *121* (50), 11928−11929.

(42) Keiper, S.; Vyle, J. S. Reversible photocontrol of deoxyribozyme-catalyzed RNA cleavage under multiple-turnover conditions. *Angew. Chem., Int. Ed.* **2006**, *45*, 3306−3309.

(43) Zhang, L.; Zhang, X.; Feng, P.; Han, Q.; Liu, W.; Lu, Y.; Song, C.; Li, F. Photodriven regeneration of G-quadruplex aptasensor for sensitively detecting thrombin. *Anal. Chem.* **2020**, *92* (11), 7419−7424.

(44) Yang, Y.; Endo, M.; Hidaka, K.; Sugiyama, H. Photo-controllable DNA origami nanostructures assembling into predesigned multiorientational patterns. *J. Am. Chem. Soc.* **2012**, *134*, 20645−20653.

(45) Liang, X.; Mochizuki, T.; Asanuma, H. A Supra-photoswitch involving sandwiched DNA base pairs and azobenzenes for light-driven nanostructures and nanodevices. *Small* **2009**, *5*, 1761−1768.

(46) Tanaka, F.; Mochizuki, T.; Liang, X.; Asanuma, H.; Tanaka, S.; Suzuki, K.; Kitamura, S.; Nishikawa, A.; Ui-tei, K.; Hagiya, M. Robust and photo controllable DNA capsules using azobenzenes. *Nano Lett.* **2010**, *10*, 3560−3565.

(47) Endo, M.; Yang, Y.; Suzuki, Y.; Hidaka, K.; Sugiyama, H. Single-molecule visualization of the hybridization and dissociation of photo responsive oligonucleotides and their reversible switching behavior in a DNA nanostructure. *Angew. Chem., Int. Ed.* **2012**, *51*, 10518−10522.

(48) Zhou, M.; Liang, X.; Mochizuki, T.; Asanuma, H. A light-driven DNA nanomachine for the efficient photo switching of RNA digestion. *Angew. Chem., Int. Ed.* **2010**, *49*, 2167−2170.

(49) Willner, E. M.; Kamada, Y.; Suzuki, Y.; Emura, T.; Hidaka, K.; Dietz, H.; Sugiyama, H.; Endo, M. Single-molecule observation of the photo regulated conformational dynamics of DNA origami nanoscissors. *Angew. Chem., Int. Ed.* **2017**, *56*, 15324−15328.

(50) Kuzyk, A.; Yang, Y.; Duan, X.; Stoll, S.; Govorov, A. O.; Sugiyama, H.; Endo, M.; Liu, N. A light-driven three-dimensional plasmonic nanosystem that translates molecular motion into reversible chiroptical function. *Nat. Commun.* **2016**, *7*, No. 10591.

(51) Han, D.; Huang, J.; Zhu, Z.; Yuan, Q.; You, M.; Chen, Y.; Tan, W. Molecular engineering of photo responsive three-dimensional DNA nanostructures. *Chem. Commun.* **2011**, *47*, 4670−4672.

(52) Chandrasekaran, A. R.; Abraham Punnoose, J.; Valsangkar, V.; Sheng, J.; Halvorsen, K. Integration of a photocleavable element into DNA nanoswitches. *Chem. Commun.* **2019**, *55*, 6587−6590.

(53) Mok, A. K.; Kedzierski, N. A.; Chung, P. N.; Lukeman, P. S. Positional photocleavage control of DNA-based nanoswitches. *Chem. Commun.* **2011**, *47*, 4905−4907.

(54) Nakamura, S.; Hashimoto, H.; Kobayashi, S.; Fujimoto, K. Photochemical acceleration of DNA strand displacement by using ultrafast DNA photo-crosslinking. *ChemBioChem.* **2017**, *18*, 1984−1989.

(55) Liang, X.; Nishioka, H.; Takenaka, N.; Asanuma, H. A DNA nanomachine powered by light irradiation. *ChemBioChem.* **2008**, *9*, 702−705.

(56) Škugor, M.; Valero, J.; Murayama, K.; Centola, M.; Asanuma, H.; Famulok, M. Orthogonally photocontrolled non-autonomous DNA walker. *Angew. Chem., Int. Ed.* **2019**, *58*, 6948−6951.

(57) Lohmann, F.; Ackermann, D.; Famulok, M. Reversible light switch for macrocycle mobility in a DNA rotaxane. *J. Am. Chem. Soc.* **2012**, *134*, 11884−11887.

(58) Willner, E. M.; Kamada, Y.; Suzuki, Y.; Emura, T.; Hidaka, K.; Dietz, H.; Sugiyama, H.; Endo, M. Single-molecule observation of the photoregulated conformational dynamics of DNA origami nanoscissors. *Angew. Chem., Int. Ed.* **2017**, *56*, 15324−15328.

(59) Fichte, M. A.; Weyel, X. M.; Junek, S.; Schafer, F.; Herbivo, C.; Goeldner, M.; Specht, A.; Wachtveitl, J.; Heckel, A. Three-dimensional control of DNA hybridization by orthogonal two-color two-photon uncaging. *Angew. Chem., Int. Ed.* **2016**, *55*, 8948−8952.

(60) Jain, K.; Ramanan, V.; Schepers, A. G.; Dalvie, N. S.; Panda, A.; Fleming, H. E.; Bhatia, S. N. Development of Light-activated CRISPR using guide RNAs with photocleavable protectors. *Angew. Chem., Int. Ed.* **2016**, *55*, 12440−12444.

(61) Tohgasaki, T.; Shitomi, Y.; Feng, Y.; Honna, S.; Emura, T.; Hidaka, K.; Sugiyama, H.; Endo, M. A photocaged DNA nanocapsule for controlled unlocking and opening inside the cell. *Bioconjugate Chem.* **2019**, *30*, 1860−1863.

(62) Liu, M.; Jiang, S.; Loza, O.; Fahmi, N. E.; Sulc, P.; Stephanopoulos, N. Rapid photoactuation of a DNA nanostructure using an internal photocaged trigger strand. *Angew. Chem., Int. Ed.* **2018**, *57*, 9341−9345.

(63) Rajendran, A.; Endo, M.; Katsuda, Y.; Hidaka, K.; Sugiyama, H. Photo-cross-linking-assisted thermal stability of DNA origami structures and its application for higher-temperature self-assembly. *J. Am. Chem. Soc.* **2011**, *133*, 14488−14491.

(64) Tagawa, M.; Shohda, K.; Fujimoto, K.; Suyama, A. Stabilization of DNA nanostructures by photo-cross-linking. *Soft Matter* **2011**, *7*, 10931−10934.

(65) Gerling, T.; Kube, M.; Kick, B.; Dietz, H. Sequence-programmable covalent bonding of designed DNA assemblies. *Sci. Adv.* **2018**, *4*, No. eaau115.

(66) Hong, F.; Jiang, S.; Lan, X.; Narayanan, R. P.; Šulc, P.; Zhang, F.; Liu, Y.; Yan, H. Layered- crossover tiles with precisely tunable angles for 2D and 3D DNA crystal engineering. *J. Am. Chem. Soc.* **2018**, *140*, 14670−14676.